INVESTIGATION OF COMBINED HEAT TRANSFER AND LAMINAR FLUID FLOW IN TWO AND THREE DIMENSIONAL DUCTS WITH AN OPEN CAVITY

Çisil TİMURALP* and Zekeriya ALTAÇ**

Department of Mechanical Engineering, Eskisehir Osmangazi University
ESOGU MeselikYerleskesi, Eskisehir 26480, Turkey
E-mail: *cisil@ogu.edu.tr, **zaltac@ogu.edu.tr

Abstract: In this study, developing combined forced and natural convection heat transfer and fluid flow in a duct with an open cavity are numerically studied using two- and three-dimensional models of various cavity size and flow induced parameters. The left wall of the cavity is isothermal while all other walls, including duct walls, are assumed to be adiabatic. Air (Pr=0.71) flows through the duct. The geometrical parameters used in this work are the cavity width to cavity height ratio (0.5≤W/D≤2), and the channel height to cavity height ratio (0.25≤H/D≤2). The flow induced parameters consists of the Reynolds number (Re) and the Richardson number (Ri). Re=10, 100, 200 and Ri=0.01, 0.1, 1 and 10 cases are considered in the study. The effects of the geometrical parameters of the cavity as well as the flow parameters on the fluid flow patterns and the temperature distribution (isotherms) were analyzed. The mean Nusselt number over the isothermal wall of the cavity was computed, and the effects of Richardson and Reynolds numbers, cavity aspect ratio and relative duct dimensions on the heat transfer were investigated. The results show that for all Re numbers, as the Richardson number increases, the air circulation becomes stronger inside the cavity. The flow inside the cavity for Ri>1 and Re>100 becomes three-dimensional. Based on the 2D and 3D numerical simulations, using the computed mean Nusselt numbers, correlations were developed.
Keywords: Natural, Forced convection, Combined flow, Three-dimensional simulation, Open cavity.

AÇIK OYUK İÇEREN KANALLARDA BİLEŞİK ISI TRANSFERİ VE LAMİNAR AKIŞIN İKİ VE ÜÇ BOYUTLU OLARAK İNCELENMESİ

Özet: Bu çalışmada, zorlanmış ile doğal taşınımın birlikte geliştiği, açık oyuk içeren bir kanalda ısı transferi ve akışkan akışı, çeşitli oyuk boyutlarıve akışa etkileyen parametrelerin cinsinden, iki- ve üç-boyutlu modellerle sayısal olarak incelenmiştir.Oyuğun sol duvarı izotermal olarak tutulurken, kanal duvarları da dâhil olmak üzere diğer tüm duvarlar adyabatik kabul edilmiştir. Kanal boyunca hava (Pr = 0.71) akışı sağlanmaktadır. Bu çalışmada kullanılan geometrik parametreler, oyuk genişliğinin ile oyuk yüksekliğine oranı (0.5≤W/D≤2) ve kanal yüksekliğinin oyuk yükseklik oranı (0.25≤H/D≤2)'dır. Akışa bağlı parametreler, Reynolds sayısı (Re) ve Richardson sayısından (Ri) oluşmaktadır. Çalışmada Re=10, 100, 200 ve Ri=0.01, 0.1, 1 ve 10 değerleri göz önüne alınmıştır. Oyuğun geometrik parametrelerinin ve akış parametrelerinin akış üzerindeki etkileri ile sıcaklık dağılımı (izotermler) analiz edilmiştir. Ortalama Nusselt sayısı, oyuğun izotermal duvarı üzerinden hesaplanmış olup; Richardson ve Reynolds sayılarının, oyuk en/boy oranının ve bağıl kanal boyutlarının ısı transferi üzerindeki etkileri araştırılmıştır. Çalışma sonuçları, tüm Reynolds sayıları için, Richardson sayısı arttıkça, oyuk içindeki hava sirkülasyonu daha güçlü hale gelmiştir.2B ve 3B sayısal simülasyonların sonuçlarına dayanarak hesaplanan ortalama Nusselt sayıları kullanılarak korelasyonlar geliştirilmiştir.
Anahtar Kelimeler: Doğal, Zorlanmış taşınım, Birlikte akış, Üç-boyutlu simülasyon, Açık oyuk.

NOMENCLATURE

D	Cavity height [m]	T	Temperature [K]
g	Earth's gravitational acceleration [m/s²]	T_0	Inlet fluid temperature [K]
Gr	Grashof number [=$g\beta\Delta T H^3/\nu^2$]	T_h	Hot wall temperature [K]
H	Duct height [m]	U_0	Inlet velocity [m/s]
Nu	Nusselt number	V	Dimensionless velocity
P	Pressure [Pa]	W	Cavity width [m]
Pr	Prandtl number [=ν/α]	k	Thermal conductivity [W/mK]
Re	Reynolds number[=$U_0 H/\nu$]	h	Convective heat transfer coefficient [W/m²K]
Ri	Richardson number [=Gr/Re^2]		

Greek symbols

ρ   Fluid density[kg/m^3]
α   Thermal diffusivity [m/s^2]
ν   Kinematic viscosity [m/s^2]
β   Volumetric thermal expansion coefficient [K^{-1}]

INTRODUCTION

Numerous studies on the convective heat transfer in an enclosure have been studied because of its wide application areas. Investigation of mixed convection of flow and heat transfer in a duct with an open cavity has also attracted attention and studied mostly numerically in recent decades due to its importance in many engineering applications such as cooling of electronic equipment, collection of solar energy, etc.

Most of the studies encountered on mixed natural and forced convection in the literature involve the numerical modeling of the rectangular cavity whose top wall is moving at a constant speed (lid-driven cavity) (Erturk et.al.,2005; Freitas and Street, 1988; Iwatsu and Hyun, 1995; Khanafer and Chamkha,1999; Moallemi and Jang, 1992; Mohamad and Viskanta,1991,1995; Prasad and Koseff,1996; Sharif, 2007); however, the studies which involve cavities heated from vertical or bottom walls placed below a fluid stream are relatively few. Some studies involving open cavity with the presence of discrete heaters, constant heat flux etc. were also pursued to observe the effects of fluid flow and heat transfer on the electronic components (Muftuoglu and Bilgen, 2008; Aminossadati and Ghasemi 2009). Chang and Tsay (2001) numerically studied the natural convection in an enclosure with a heated backward step to investigate the effects of the Rayleigh and Prandtl numbers as well as the size of the enclosure on the flow structure and heat transfer characteristics.The study revealed that the extent of heat transfer enhancement increased with decreasing Rayleigh number. Manca et al. (2006, 2008) experimentally investigated mixed convection and opposing mixed convection in a duct with an open cavity below a horizontal duct. Also some experimental and numerical studies have been conducted with natural convection in two-dimensional enclosures (Calcagnietal., 2005; Das et al., 2002; Ishihara et al., 2002). Aydın et al. (1999) analyzed natural convection of air in enclosure heated from one side and cooling from the top numerically to observe the effects of the Rayleigh number and the aspect ratio on the flow pattern. It was observed that the effect of Rayleigh number on heat transfer was more significant when the enclosure was shallow and the Ra number was high, and when the enclosure was tall, the influence of aspect ratio was stronger. Leong et al. (2005) numerically studied mixed convection in a horizontal channel for $1 \leq Re \leq 200$, $0 \leq Gr \leq 10^6$ and $0.5 \leq D/W \leq 4$. They observed that Reynolds number and Grashof number controlled the flow pattern and the flow became unstable in the mixed convection regime. Manca et al. (2003) investigated numerically the effect of heated wall

position on mixed convection in two-dimensional horizontal channel with an open cavity. They studied streamlines and isotherms for Re=100 and 1000 and Ri=0.1 and 100. The results showed that the mean Nusselt number and the maximum temperature were obtained in the opposing forced flow configuration. Rahman et al. (2012) numerically studied flow and heat transfer in a duct with a cavity heated from different sides subjected to a magnetic field. For specified Pr=0.7 and Re=100 conditions, a constant magnetic field is imposed to the duct. Basak et al. (2009) studied mixed convection flows within a square cavity heated from bottom. They obtained numerical solutions for various values of $1 \leq Re \leq 100$, $10^3 \leq Gr \leq 10^5$ and $0.015 \leq Pr \leq 10$.The flow patterns indicated that the natural or forced convection is based on both the parameters Richardson and Pr numbers. For Pr=7, $1 \leq Gr \leq 4000$, $50 \leq Re \leq 1000$, Sidik et al. (2014) numerically simulated mixed convection for fluid with particle laden flow in an open cavity with an aspect ratio of 4 which is heated from below. This study illustrates the variations in the Grashof number made a remarkable difference in the observed flow pattern and cleaning efficiency. Selimefendigil and Yurddas (2012) investigated using 2D numerical model for the mixed convection in a channel with a cavity heated from below and left vertical walls for pulsating flow for $0.1 \leq Ri \leq 100$, $300 \leq Re \leq 800$ and for Strouhal numbers from 0.25 to 1. Brown and Lai (2005) studied numerically combined heat and mass transfer from a 2D horizontal channel with an open cavity heated from below for Pr =0.7, $1 \leq Re \leq 1000$, $0 \leq Gr \leq 10^6$ and $0.1 \leq Le \leq 10$. Based on the two-dimensional numerical simulations, correlations for the entire convection regime, from natural, mixed, to forced convection, were proposed. Burgos et. al. (2016) numerically studied steady and unsteady laminar flow in a duct with a cavity heated from below for $50 \leq Re \leq 1000$ and $0.01 \leq Ri \leq 10$. They observed that the analysis of the unsteady regime revealed a very rich phenomenology where the geometry of the problem couples with the oscillatory thermal instability.

Recently flow of nanofluids in a duct with an open cavity has attracted some attention due to technological applications. Abdellahoum et al. (2015) numerically studied 2D turbulent forced convection of Al_2O_3 nanofluid over a heated cavity in a horizontal duct and investigated the effects of Re number ($10^4 \leq Re \leq 10^5$) and nanoparticles concentration ($0 \leq \phi \leq 4\%$) on the heat transfer and flow characteristics. As a result, the mean Nusselt number increased with the volume fraction of nanoparticles for the whole range of Re number. And also Pack and Cho viscosity model gave maximum friction and heat transfer. Mehrez et al. (2013) numerically investigated mixed convection and entropy generation of nanofluids flow in an open cavity heated from below for $1 \leq AR \leq 2$, $100 \leq Re \leq 500$, $0.05 \leq Ri \leq 1$ and solid volume fraction of nanoparticles up to 10%. It was found that the heat transfer and the entropy generation increased with increasing Re and Ri numbers, and volume fraction of nanoparticles. In a follow up study, Mehrez et al. (2015) numerically studied entropy

generation and mixed convection heat transfer of Cu–water nanofluid flow in an inclined open cavity uniformly heated from the left wall. The investigation is carried out for a wide range of inclination angles of the cavity and the range of nanoparticle volume fractions up to 6%, for $100 \leq Re \leq 500$ while the Grashof number was fixed at 10^4. The results show that for all inclination angles, the enhancement rate of heat transfer is higher than the increase rate of entropy generation.

Numerical simulations involving three-dimensional models are relatively rare. Stiriba et al. (2010) investigated numerically the effects of mixed convective flow over a three-dimensional cavity which is situated at the bottom of a horizontal channel and heated from right cavity wall. A parametric study is performed for $10^3 \leq Gr \leq 10^6$ and $100 \leq Re \leq 1000$. For high Re and Ri numbers the natural convection was involved in and pushed the recirculation zone further upstream. Pallares et al. (1996) studied natural convection in a cubical cavity heated from below for $3500 \leq Ra \leq 10^4$. They reported that the effect of the Rayleigh number and the type of flow structure on heat transfer rates at the top and bottom plates. The heat transfer and fluid flow characteristics of laminar flow in an open cavity heated from below was carried by Stiriba et al. (2013). The effects of Reynolds and Richardson number on the flow in the duct and inside the cavity are studied for $100 \leq Re \leq 1500$ and $0.001 \leq Ri \leq 10$. It was observed that the flow became steady at both low Ri and Re number, and as Ri number was increased, the buoyancy became stronger and part of the heated fluid moved to the left side wall. Abdelmassih et al. (2016) numerically and experimentally studied 3D steady and unsteady mixed convection in a cubical open cavity heated from below for $100 \leq Re \leq 1500$ and $0.1 \leq Ri \leq 10$. The results show that alternate flow ejections persist for all the Reynolds values analyzed.

The interaction between a flowing external stream and the buoyancy driven flow induced by a heated surface from cavity walls leads to the possibility of complex flows. Therefore it is important to understand the heat transfer characteristics of a mixed convection in such configurations. Correlations involving a wide range of design parameters are practically nonexistent. The objective of this study is to investigate two-dimensional and three-dimensional combined forced and natural convection heat transfer and fluid flow in an open cavity (heated from the left wall) which is located below a horizontally configured duct. The geometrical duct parameters, duct height to cavity height (H/D) and cavity width to cavity height (W/D), and flow parameters, Reynolds and Richardson numbers, are varied in a wide range, and the streamlines as well as isotherms are examined qualitatively. A basic quantitative parameter which is the mean Nusselt number was computed as an average over the heated wall surface area. Finally, based on 2D and 3D numerical trials two correlations are developed.

PHYSICAL PROBLEM AND MATHEMATICAL FORMULATION

A horizontal square duct of H×H in cross section and 8×W in length is considered. A cavity with a width W and height D is placed at bottom at a distance 4×W away from the entrance of the duct. The geometry and the coordinate system as well as the geometric variables used in this study are illustrated in Fig. 1.
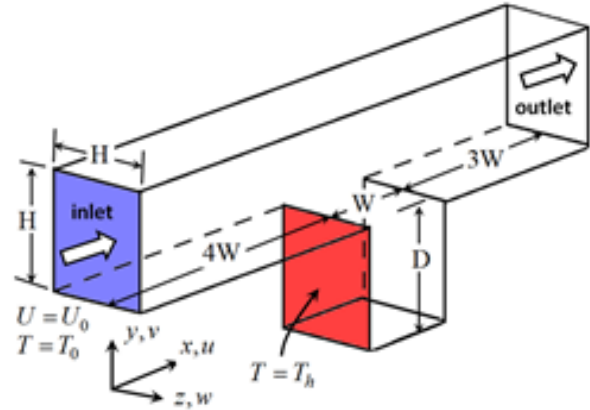
Figure 1. Schematic diagram of the geometry

In this study, the radiative heat exchange is neglected and the thermo-physical properties are assumed to be constant except for the density for which the Boussinesq approximation is used. The working fluid is air (Pr=0.71), and it enters to the duct with a uniform velocity U_0 with ambient temperature T_0. The temperature and flow fields are allowed to develop within the enclosure. Also the flow is assumed to be steady, laminar and incompressible. Constant temperature is applied to the left cavity wall while all other remaining walls, including those of the duct, are assumed to be adiabatic.

Under these assumptions the governing equations can be stated as; for the continuity

$$\nabla \cdot \mathbf{V} = 0 \qquad (1)$$

for the momentum equations

$$(\mathbf{V} \cdot \nabla)\mathbf{V} = -\frac{1}{\rho}\nabla P + \nu \nabla^2 \mathbf{V} - g\beta(T - T_0)\mathbf{j} \qquad (2)$$

and for the energy

$$(\mathbf{V} \cdot \nabla)T = \alpha \nabla^2 T \qquad (3)$$

where $\mathbf{V}$ is the velocity, ρ is the density, P is the pressure, ν is the kinematic viscosity, α is the thermal diffusivity, β is the thermal expansion coefficient, T is the temperature and $\mathbf{j}$ is the unit vector depicting y-direction. Due to the physical phenomenon taking place, the dimensionless numbers encountered here are Prandtl, Reynolds, Grashof and Richardson numbers which are defined as $Pr = \nu/\alpha$, $Re = U_0 H/\nu$, $Gr = g\beta\Delta TH^3/\nu^2$ and $Ri = Gr/Re^2$ respectively.

The boundary conditions (for the general 3D model) can be stated as follows:

duct inlet $T = T_0$, $u = U_0$, $v = w = 0$,

duct outlet $\dfrac{\partial u}{\partial x} = \dfrac{\partial v}{\partial x} = 0$, $\dfrac{\partial T}{\partial x} = 0$, $P = 0$

adiabatic walls $\dfrac{\partial T}{\partial n} = 0$, $u = v = w = 0$

heated cavity wall $T = T_h$, $u = v = w = 0$

where T_0 and T_h are the inlet (ambient) and the hot wall temperatures, respectively; P is the gauge pressure at the pressure outlet, U_0 is the fluid velocity at the entry of the duct and **n** denotes the direction normal to the wall.

Once the temperature field is resolved, by equating convection heat flux to that of the conduction heat flux, the local convective heat transfer coefficient at every face nodes are computed. Then the mean heat transfer coefficient and Nusselt number is computed over the isothermal heated surface area according to

$$\bar{h} = \frac{1}{A_h} \iint_{A_h} h \, dA$$

(4)

$$\overline{Nu} = \frac{\bar{h}H}{k} = \frac{1}{A_h} \iint_{A_h} Nu \, dA$$

(5)

where k is the conductivity of air, A_h is the heated surface area, $\bar{h}$ and $\overline{Nu}$ are the mean heat convection transfer coefficient and the mean Nusselt number.

NUMERICAL SOLUTION

The continuity, momentum and energy equations are solved using Fluent 6.3®(2003) where Boussinesq approximation is employed for the density variations. In the discretization of the convection terms, the second order upwind and as for the solution algorithm SIMPLE is used. In the numerical simulations, the cavity aspect ratio (W/D) and duct height to cavity height ratio (H/D) are varied for 0.5≤W/D≤2 and 0.25≤H/D≤2 intervals. Richardson number which is a measure of natural convection heat transfer rate to that of forced convection is varied from 0.01 to 10 while, in this study, the Reynolds numbers for 10, 100 and 200 are investigated.

Table 1. Comparison of the computed Nusselt numbers with published results.

Ri=1, Re=10		Ri=0.01, Re=100		Ri=0.1, Re=100		Re=0.1, Re=1000	
Leong, 2005	Present	Leong, 2005	Present	Stiriba 2008	Present	Stiriba 2008	Present
2.209	2.309	3.837	4.006	3.2	2.956	7.8	7.157

Table 2. Grid sensitivity analysis for W/D=1 case.

Grid size	Ri=0.01 Re=100	Ri=0.01 Re=200	Ri=0.1 Re=100	Ri=0.1 Re=10
10^3	2.357	2.744	2.470	1.569
20^3	2.413 (2.3%)	2.806 (2.21%)	2.527 (2.25%)	1.597 (1.75%)
40^3	2.449 (1.47%)	2.830 (0.85%)	2.563 (1.40%)	1.617 (1.24%)
50^3	2.456 (0.28%)	2.822 (0.28%)	2.571 (0.31%)	1.624 (0.43%)

To validate the accuracy of Fluent® solutions with respect to the grid configuration and to ensure grid independent solutions, the numerical solutions are obtained using various grid configurations in the computational domain. First, to determine the accuracy of the present study, the numerical solutions for 2D-model are compared with those of available numerical studies in the literature. The comparative results are presented in Table 1. It is observed that presented solutions fairly agree with the published literature. The numerical simulation results and relative errors with respect to the mean Nusselt numbers for W/D=1 and four different grid configurations (10^3, 20^3, 40^3 and 50^3) are depicted in Table 2 to determine the grid independency. The grid is further clustered near the walls in order accurately to obtain the velocity and temperature gradients. It is determined that with the relative errors below 0.5% as depicted in Table 2,

configuration with 50^3 is the optimum grid configuration. Since flow is laminar, it is observed that the grid structure influences the mean Nusselt results relatively less.

RESULTS AND DISCUSSION

The flow field (streamlines) and temperature distributions (isotherms) for the 2D and 3D studies are produced for each simulation. These distributions are compared and analyzed with respect to the dimensionless parameters (Re and Ri) and geometrical parameters (W/D and H/D) considered.

Two-Dimensional Analysis

For Ri=0.01, H/D=0.5 and Re=10, the variations of streamlines and isotherms with respect to W/D aspect
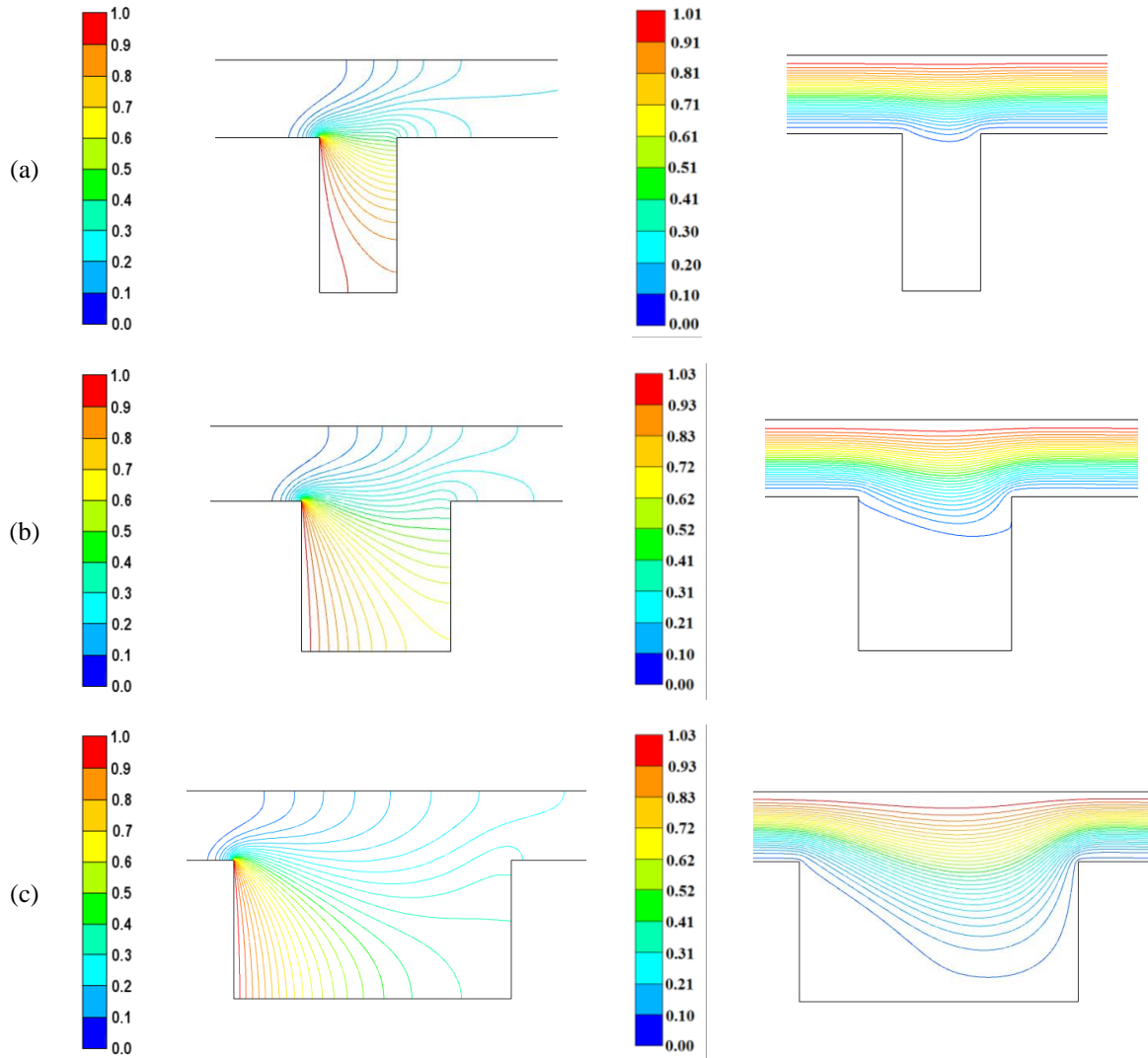
Figure 2. The effect of aspect ratios on isotherms on the left hand side (LHS) and streamlines on the right hand side (RHS) for Ri=0.01, H/D=0.5 and Re=10.(a) W/D=0.5, (b) W/D=1, (c) W/D=2

ratio are depicted in Fig. 2. For a slender cavity (W/D=0.5), the streamlines display almost a linear path on the upper portion of the duct while the moving fluid adjacent to the cavity-top depicts a small dip into the cavity. As a result of this, the fluid inside the cavity remains relatively undisturbed which yields an increase in the temperature of the cavity. The isotherms indicate that the heat transfer mechanism taking place in the cavity is mostly governed by conduction. The thermal boundary layer starting from the top of the cavity encompasses almost the whole cavity. Due to the formation thick thermal boundary layer, hot wall surface yields small temperature gradients as a result the convection heat transfer from the hot cavity wall becomes insignificant. As the aspect ratio W/D increases, the surface area of the cavity open-top surface area facilitates the entrance of the fluid into the cavity (Figs. 2b and 2c) which in turn disturbs relatively inactive fluid. For W/D=1, the region below the bottom streamline in the cavity, the fluid is trapped inside the cavity (Fig. 2c). As W/D increases, the thermal boundary layer shrinks towards the heated wall, the

streamlines are stacked closer thereby the temperature gradients as well as the convection heat transfer rates are increased. However, this increase is still not significant enough to overcome the present conduction mode. For Ri=0.01, W/D=1 and Re=200, the variations of streamlines and isotherms with respect to H/D (0.25≤H/D≤2) ratio are depicted in Fig. 3. In Fig. 3a, the cavity height is 4 times larger than the duct height, the isotherms concentrate on the left wall yielding higher temperature gradients. There is a strong clockwisecirculation inside the cavity which encompasses the entire cavity. The thermal boundary layer is almost symmetrical with respect to central horizontal line where it becomes the thinnest. At the upper portion of the cavity, the isotherms indicate that due to strong clockwise circulations, the fluid escapes the cavity and drifts in the main flow direction along the duct (Fig. 3a) which is consisted with the streamlines.
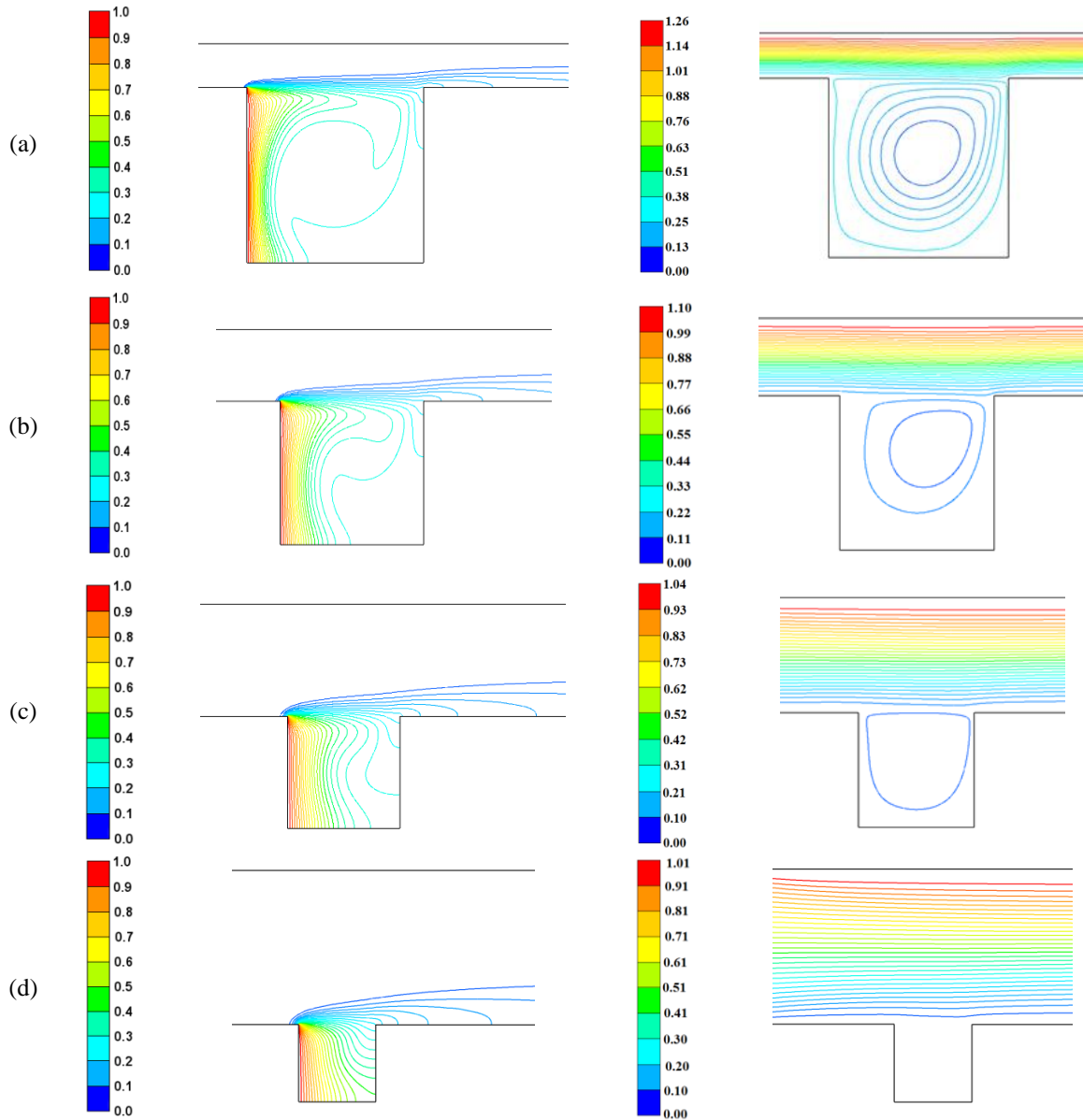
Figure 3. The effect of H/D on isotherms (LHS) and streamlines (RHS) for W/D=1, Ri= 0.01, Re=200, (a) H/D=0.25, (b) H/D=0.5, (c) H/D=1, (d) H/D=2

As H/D is further increased, the strength of the circulation in the cavity is reduced due to fluid volume flowing in the cavity. The circulation center shifts slightly to the northeast of the cavity. As a result of all these, both hydrodynamic and thermal boundary layer thicknesses are increased in comparison to H/D=0.25 case. The fact that some of the hot air escapes and fresh cold air enters the cavity, the natural circulation becomes evident. As H/D is further increased, as depicted in Figs. 3c and 3d, due to smaller cavity height or shallower cavity, the amount of air leaking from the cavity increases leaving no change for natural circulation cycle to be fully completed. Due to strong duct flow (Re=200), as air rises to the top surface level, it is transported away from the cavity in the main flow direction (Fig. 3d).For Ri=0.01, W/D=1 and H/D=0.25, the variations of streamlines and isotherms with respect to Reynolds number (Re=10, 100, 200) are depicted in

Fig. 4. In Fig. 4a, for Re=10, the fluid velocity is considerably small. The rising air due to heat input from the hot wall inthe cavity has the potential to fill the upper portion of the cavity including the corresponding duct section. The streamlines follow a strong curved pattern on the right upper corner of the cavity sweeping the fluid yielding higher fluid temperatures in the downstream of the duct. The thermal boundary layer, due to relatively weak and small circulation, is thick with small temperature gradients at the hot surface, and thus the convection heat transfer rate is significantly small. In Fig. 4b, for Re=100, the fluid velocity is significantly higher than the previous case. Frictional interaction between the fast moving fluid inside the duct and the fluid at the top surface of the cavity creates a stronger clockwise circulation within the cavity. The influence of natural convection is evident. As the circulation gains strength with
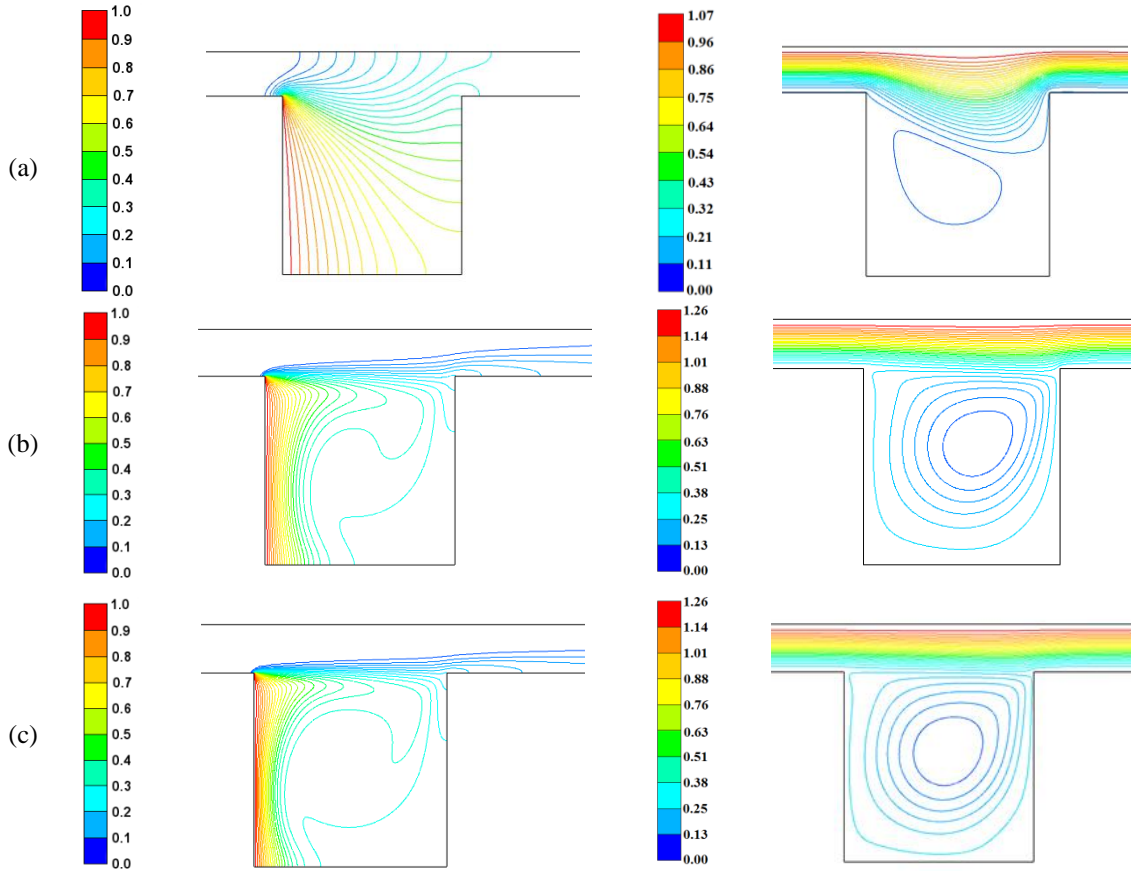
Figure 4. The effect of Reynolds number on isotherms (LHS) and streamlines (RHS) for W/D=1, H/D=0.25 and Ri=0.01, (a) Re=10; (b) Re=100; (c) Re=200.

increasing Re number, the isotherms shrink tighter towards the heated wall yielding increased heat transfer rates; however, during the clockwise circulation of the cavity fluid, some of the rising hot air leak out of the cavity and drifts away along the downstream of the duct. In Fig. 4c, for Re=200, natural circulation caused by buoyant flow expands towards all three walls encompassing the whole cavity. The isotherms are clustered on the hot left wall further squeezing thermal boundary layer yielding steeper temperature gradients in comparison to Re=100 (Fig. 4b) case. Since Re=100 and Re=200 cases involve faster moving duct fluid, the streamlines and isotherms of the two cases are very much similar (Figs. 4b and 4c) in comparison to that of Re=10 which yields much slower axial velocity in the duct.

To observe the effect of Richardson numbers on the flow and heat transfer, computations for Ri=0.01, 0.1, 1 and 10 have been conducted. For Re=10, H/D=0.15 and W/D=1, the variations of streamlines and isotherms with respect to Richardson number are depicted in Fig. 5. In Fig. 5a, Ri=0.01 case, due to small Re number, the air flow into the duct is facilitated mostly from right side of the cavity because of the direction of the velocity vectors. The straight horizontal flow is influenced by rising hot air which penetrates into the cavity slightly.

Conduction heat transfer at two-thirds of the bottom region, where a weak non-uniform circulation occurs, is dominated; therefore, the thermal boundary layer covers almost the entire cavity. The streamlines above the cavity depict deviation towards northeast of the cavity due to relatively small inertia forces. For Ri=0.1 (Fig. 5b), the isotherms are similar to those of depicted in Fig. 5a, but the eddy in the cavity slightly gains strength, and the clockwise circulations spread out to extend the side walls. In Fig. 5c, for Ri=1 where the influence of the buoyancy forces increase, although fluid passing the duct slightly penetrates into the cavity at the top surface, the inertia forces are strong enough to trap most of the fluid inside the cavity. Unicellular circulation becomes stronger covering the entire cavity. It is observed that the shape of the thermal boundary layer is also distorted due to the interactions between the competing buoyancy and inertia forces. This leads to steeper temperature gradients at the bottom half of the heated wall in turn yielding higher heat transfer rates in comparison to previous cases. For Ri=10, in Fig. 5d, the streamlines and isotherms take the form of the flow in a single cavity enclosed by four walls. Natural circulation, a unicellular clockwise roll, is observed within the entire cavity leading to streamlines covering the entire cavity. Due to the flow field, the temperature gradients along the hot wall and thus the heat transfer rate are increased.
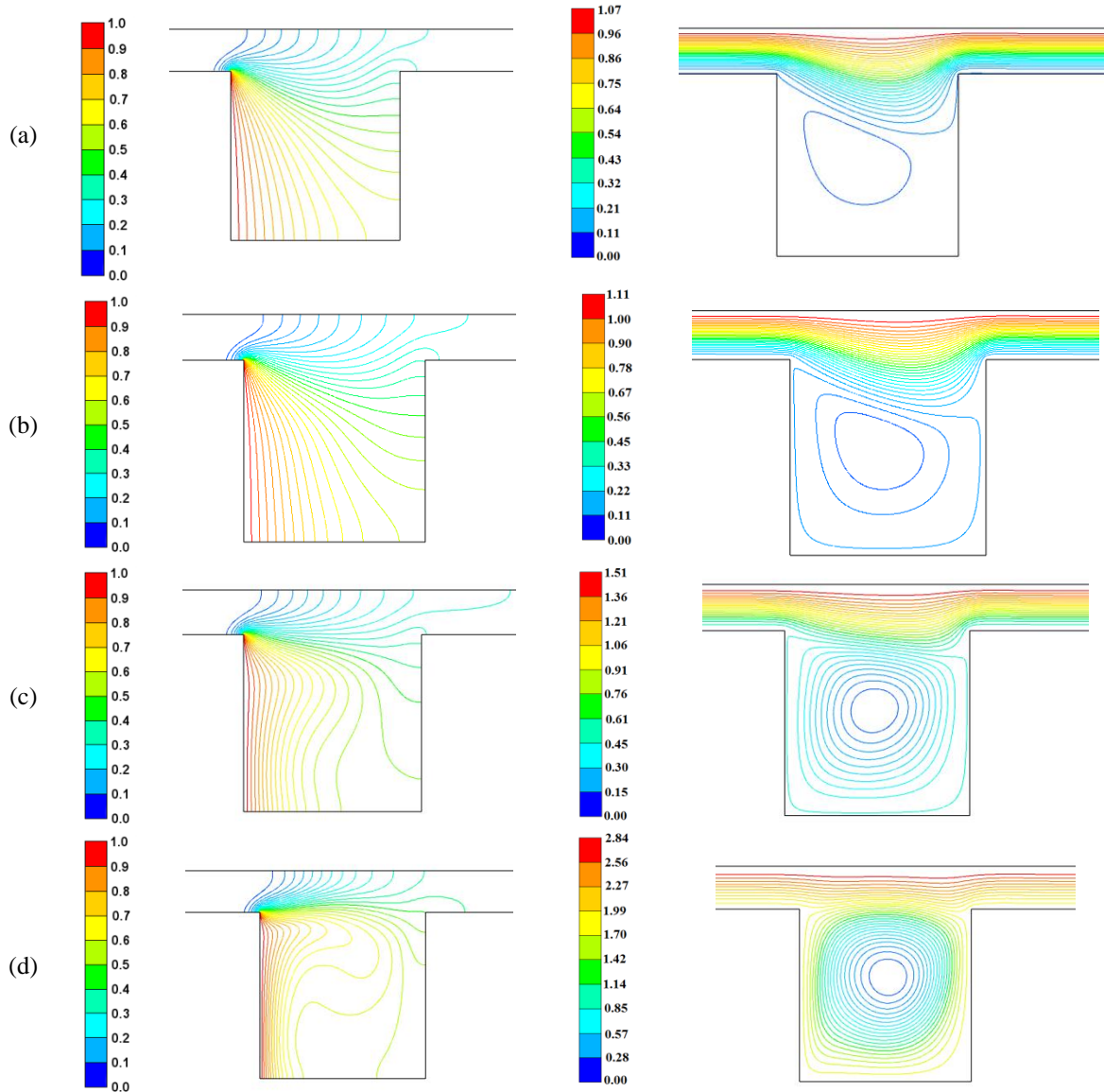
Figure 5. The effect of Richardson Number on isotherms (LHS) and streamlines (RHS) for W/D=1, H/D=0.25 and Re=10, (a) Ri=0.01; (b) Ri=0.1; (c) Ri=1; (d) Ri=10.

Three-Dimensional Analysis

For W/D=0.5 and W/D=1, the pathlines (colored by temperature) are depicted for H/D=1 and Ri=0.1, and for Re=10, 100 and 200 in Fig. 6 to observe the effect of cavity length (W) to cavity height (D) ratio. For W/D=0.5, the cavity is tall having relatively small surface area of interaction between the duct and the cavity in comparison to W/D=1 in which case the surface area is doubled. In Fig. 6a, for Re=10 and W/D=0.5, the fluids lightly penetrates into the cavity from the open top surface. The penetrating fluid is pushed upwards due to buoyancy forces while the bottom of the cavity remains relatively inactive due to a weak circulation. For W/D=1, the cavity's surface is longer or larger along the flow direction. Thus, due to competing forces, the fluid is able to achieve deeper penetration covering most of the cavity. The region occupied by the three-dimensional boundary layer decreases which leads to cooler temperatures inside the cavity because of increased motion of the fluid within the cavity. The flow at the front and back walls of the cavity is hindered due to friction between the fluid and aforementioned cavity walls. The temperature of the fluid passed cavity also increases with respect to afore the cavity due to this interaction. For Re=100 in Fig. 6b, for W/D=0.5 (LHS), the fluid flowing thru the duct does not exhibit significant penetration into the cavity; thus, the circulation in the cavity displays 2-D flow characteristics. The fluid rising from the cavity distorts pathlines above the cavity, but it soon recovers at the downstream of the duct. Relatively weak activity in the cavity, fluid temperature inside the cavity increases yielding small temperature gradients and thus small heat transfer rates.
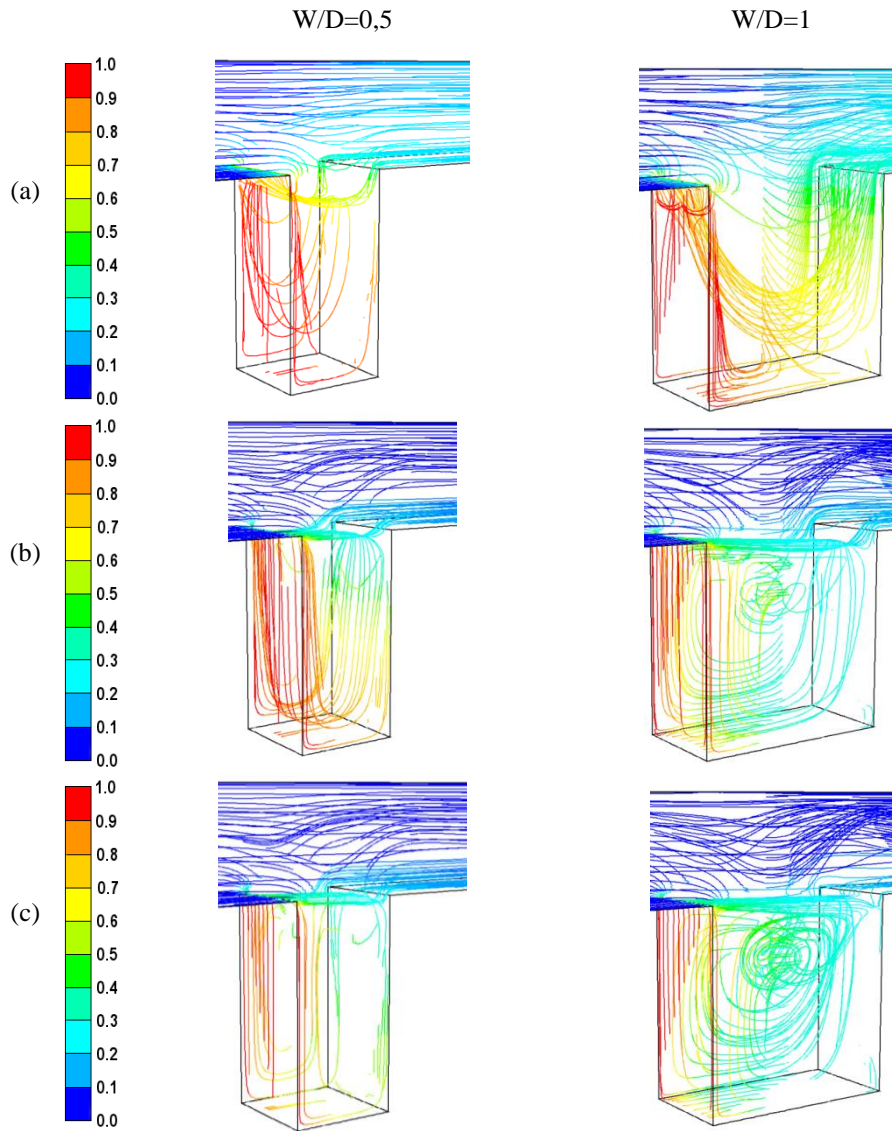
Figure 6. Pathlines (colored by temperature) for H/D=1, Ri=0.1 and W/D=0.5(LHS); W/D=1(RHS) (a) Re=10, (b) Re=100, (c) Re=200

For Re=100 and W/D=1, while the general form of the roll complies with unicellular pattern, the pathlines depict 3-D flow patterns especially at the core of the cavity. In the meantime, the flow above the cavity is further distorted and the flow later recovers to its original horizontal pattern further downstream. The motion of the fluid in the cavity is limited in the zone away from the walls where the friction forces reduce the inertia of the fluid motion. For Re=200 and W/D=0.5 in Fig. 6c, the fluid motion basically resembles those of Fig. 6b; however, the fluid, as the circulation inside the cavity gains strength, expands towards the cavity walls. For W/D=1, the circulation inside the cavity not only maintains its 3-D structure but also expands and becomes more violent leading to a better mixing within the cavity which in turn shrinks the thermal boundary layer region. This physical phenomenon increases the heat transfer rate. For H/D=0.5, 1 and 2, the pathlines (colored by temperature) are depicted for Ri=0.1, W/D=0.5 and for Re=10, 100 and 200 in Fig. 7. In Fig.

7a, for W/D=0.5, the pathlines are depict slight fluid penetration into and out of the cavity at the duct-cavity interface while fluid motion is directed upwards due to occurring density differential which also slightly distorts the flow in the duct above the cavity. The cavity becomes hotter yielding small temperature gradients at the heated wall. When the cavity height is doubled (H/D=1), the inertia forces are increased and the amount of fluid penetration into the cavity is reduced. The weak fluid circulation is basically confined to the upper portion of the cavity. The cavity temperature increases in comparison to H/D=0.5 as a result the temperature gradients at the heated wall surface decrease. This trend is maintained for H/D=2 case as well. In Fig. 7b, for H/D=0.5, the fluid velocity increases with Re number. The clockwise flow pattern in the cavity display 3D characteristics due to the inflow of fluid from the duct flow. As a result of this impact, the duct flow above the cavity is distorted which recovers at the duct downstream. For H/D=1, increased mass and inertial

H/D=0.5   H/D=1   H/D=2

(a)

(b)

(c)
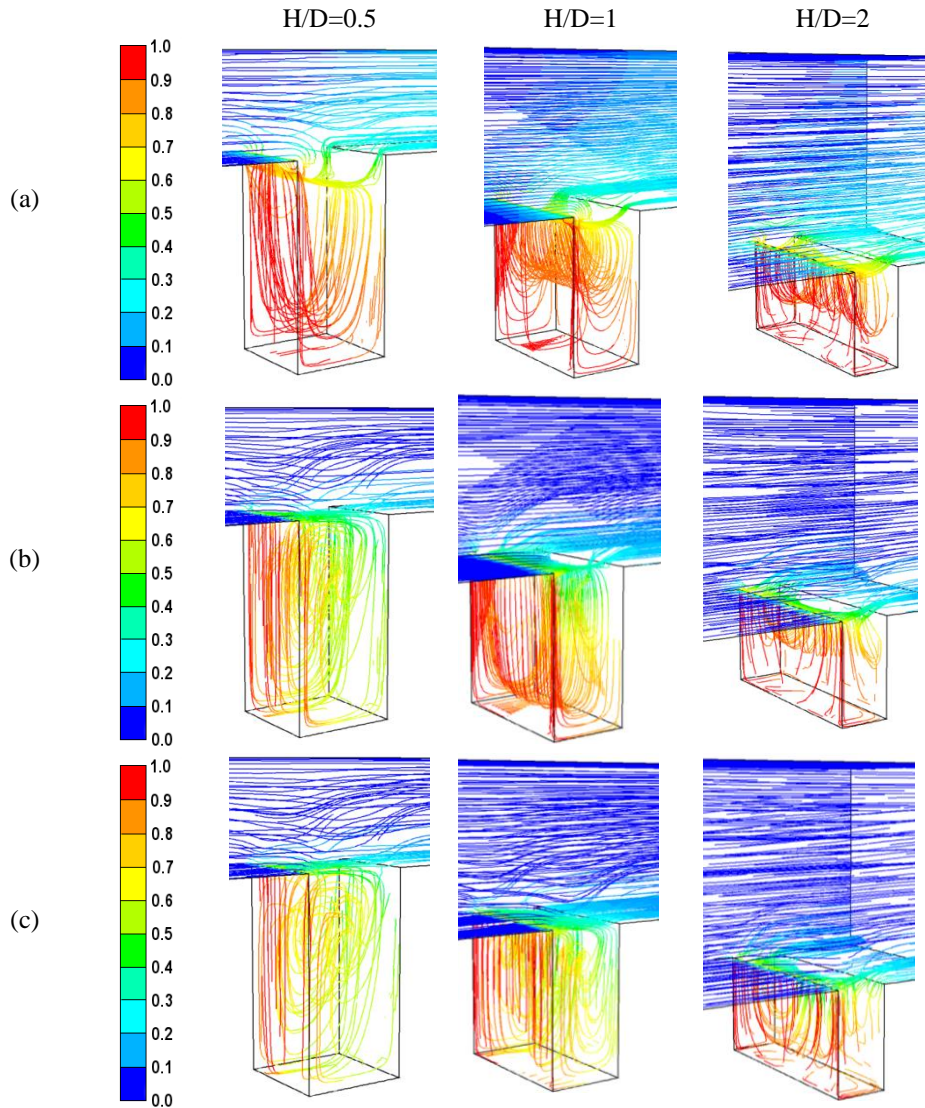
Figure 7. Pathlines (colored by temperature) for W/D=0.5, Ri=1 and H/D=0.5(1st col.); H/D=1(2nd col.); H/D=2(3rd col.) :(a) Re=10, (b) Re=100, (c) Re=200

forces created in the duct lead to smaller distortions in the fluid motion in the duct which confines the fluid inside the cavity. The flow at the interior region of the cavity depicts 2D flow patterns, but the frictional effects are clearly observed near the cavity walls. For H/D=2 in Fig. 7b, the duct height is comparatively much larger than that of the cavity. Thus the mass of the fluid is larger which leads the fluid suppression in the cavity. As a result, a weak circulation confined at the upper half of the cavity is observed. For Re=200 and H/D=0.5 (Fig. 7c), circulations with 3-D mixed-flow structures occupying the entire cavity are formed. For H/D=1, weaker yet 3-D flow patterns are formed at the upper half of the cavity, and it is relatively inactive at the lower half. For H/D=2, the pathlines of the fluid flowing inside the duct is almost linear with slight distortions above the cavity. This means that the fluid in the cavity remains trapped and circulations inside are to be expected.

In Fig. 8, the effects of the Reynolds number on the pathlines are depicted for two cases (1) H/D=0.5,

W/D=0.5, Ri=0.1 (on LHS) and (2) H/D=1, W/D=1, Ri=1 (on RHS). For Re=10 and for Case 1, a weak circulation extending to the duct level is formed. The fluid is relatively motionless at the bottom portion of the cavity. For Re=100, the duct flow partially shifts into the cavity which slams into the wall opposite of the hot wall and continues to circulate in the cavity. The clockwise circulation covers the entire cavity while the circulation generally maintains 2-D flow pattern. As a result, the size of the thermal boundary region is reduced which leads to increased heat transfer rates. For Re=200, the fluid in the cavity is active. For Case 2 in Fig. 8, due to increased top surface area of the cavity, the amount of the inflow fluid up to the top one-third of the cavity increases while creating a cellular (2-D like) fluid motion below this path; however, the circulations are not very strong because of small value of Re number. Since the fluid cannot escape the cavity, the temperatures within the circulation zone which encompasses the hot wall increase yielding small temperature gradients at the surface of the hot wall.

42
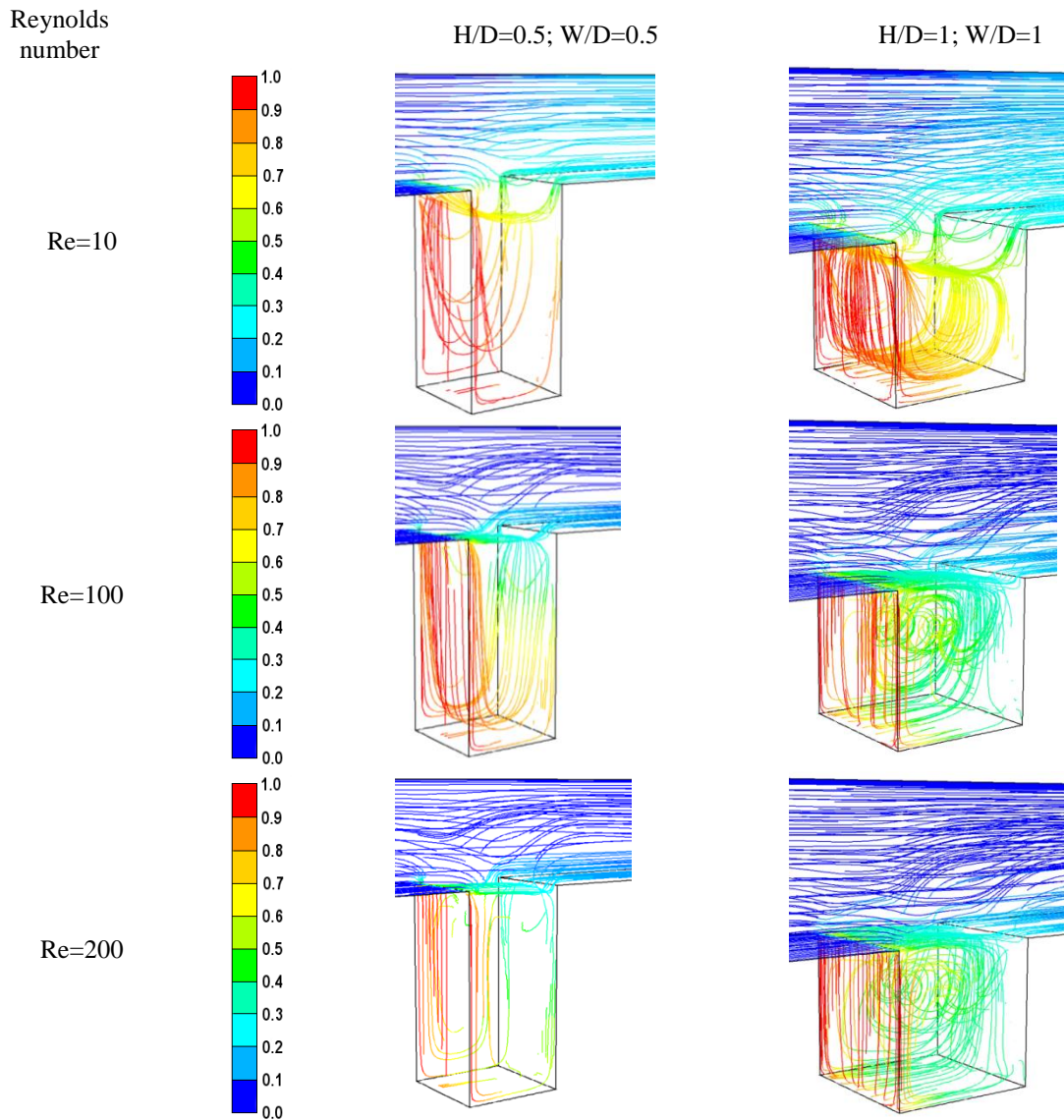
Figure 8.Pathlines (colored by temperature) for different Re numbers (LHS: H/D=0.5; W/D=0.5; Ri=0.1 RHS: H/D=1, W/D=1, Ri=1)

For Re=100, the fluid flow inside the cavity exhibiting 3-D flow patterns is violent. The flow covers the entire cavity; however, the velocity and temperature gradients are observed to be much steeper at the hot wall implying significant increase in the heat transfer rates. For Re=200, basically similar flow and heat transfer patterns are also observed here. Due to higher Reynolds number value, the mixing is more vigorous extending towards enclosing walls, and as a result, the thermal boundary layer region is much smaller.

In Fig. 9, the effects of Richardson number on the flow and heat transfer are depicted for (a) Re=10, (b) Re=200 and for H/D=1 and W/D=0.5. For Re=10, the circulation created at the upper half of the cavity extends towards the bottom wall of the cavity as Richardson number is increased. The flow structure complies with 2D flow patterns, but the effects of the fluid frictions with the walls become more pronounced with increasing Ri number. For Re=200, the flow structures depict 3-D flow patterns with features strengthening by increasing Ri number. It is noted that for Ri=10, the buoyancy

forces are strong enough to overcome inertial forces at the open top of the cavity so that rising cavity fluid causes strong distortions in the region above the cavity.

Fig. 10, using the 3D numerical simulations, the variation of the Nusselt number with the Reynolds number and H/D for Ri=0.1 and 1, and for W/D=0.5 and 1 is depicted. For Ri=0.1 and fluid flow at low Reynolds numbers (Re=10), the change in the mean Nusselt number is insignificant. For Re=10, it is observed that Nu<1 due to stagnant fluid becoming hotter in the cavity which facilitates conduction heat transfer. However, as the Reynolds number is increased, the mean Nusselt number increases with W/D for H/D>0.5 due to strengthening duct flow and increased open surface area of the cavity. For W/D=0.5 and Ri=0.1, the relative increases in mean Nusselt numbers with respect to H/D=0.5 are, respectively for H/D=1 and 2, 59% and 60% for Re=10, 56.5% and 62.1% for Re=100, and 36.3% and 57.3% for Re=200. The relative increases in the mean Nusselt numbers for W/D=1 with respect to
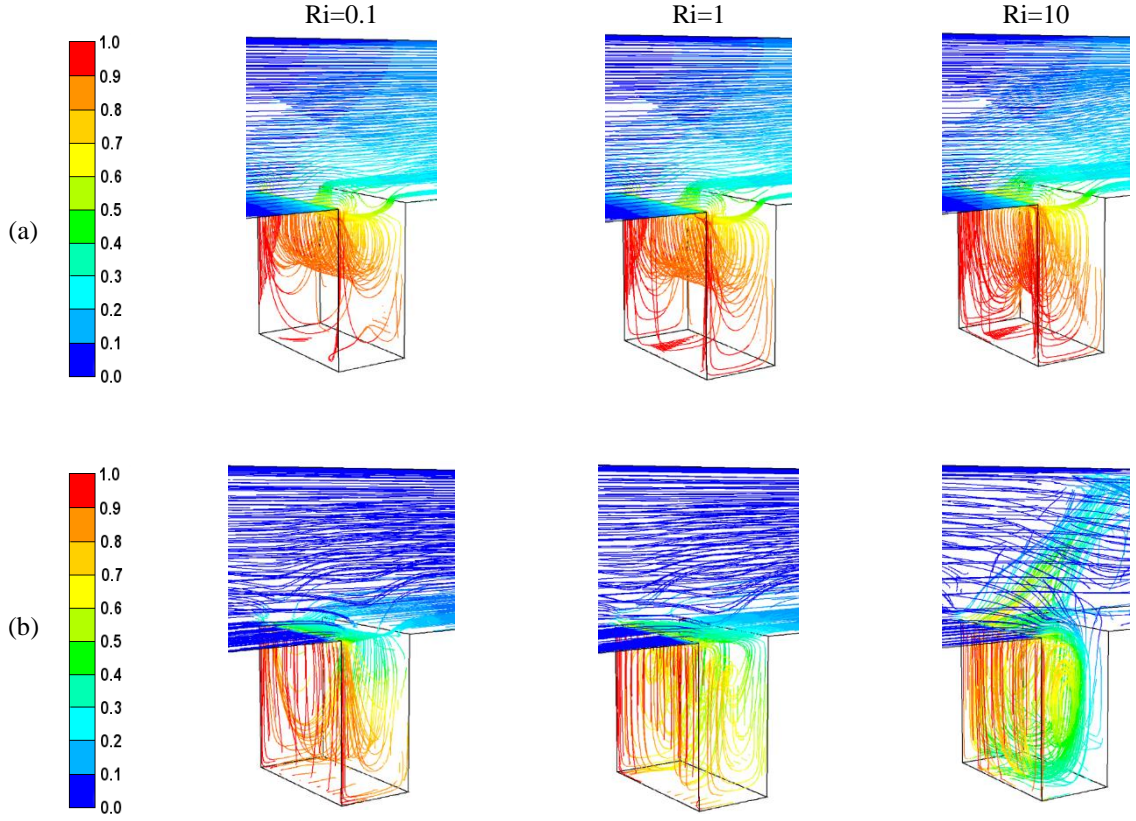
Figure 9. Pathlines (colored by temperature) for different Ri numbers H/D=1, W/D=0.5: (a) Re=10, (b) Re=200.

W/D=0.5 are 25%, 27% and 37% for Re=100 and 21.5%, 22% and 26.5% for Re=200 (Figs. 10a and 10b), respectively, for H/D=0.5, 1 and 2. In Figs.10c and 10d, the mean Nusselt number variations are depicted for Ri=1. The mean Nusselt numbers for Re=10 are identical to Ri=0.1; that is, for duct flows of low Reynolds number, the Richardson number does not have a significant effect on the heat transfer rates. On the other hand, as the Reynolds number is increased, the mean Nusselt number increases with W/D. For W/D=0.5 and Ri=1, the relative increases in mean Nusselt numbers with respect to H/D=0.5 are, respectively for H/D=1 and 2, 59% and 60% for Re=10, 25.5% and 57.1% for Re=100, and 25.5% and 38.2% for Re=200. The relative increases in the mean Nusselt numbers for W/D=1 with respect to W/D=0.5 are 24.8%, 45.1% and 44% for Re=100 and 21.5%, 25% and 35.4% for Re=200 (Figs. 10c and 10d), respectively, for H/D=0.5, 1 and 2.

It is observed that the flow in some cases can be considered two-dimensional. This phenomenon is also observed in the quantitative results depicted by the mean Nusselt numbers tabulated in Table 3. For Ri≤1, the mean Nusselt numbers are almost identical where 3D computations yield slightly larger Nu values. This is also observed for large Reynolds number flows (Re=100 and 200); however, as the Richardson number

is increased, computed Nusselt numbers from the 3D simulations are consistently smaller than those of 2D simulations. It is observed that the deviations in the mean Nusselt numbers increase with the Reynolds number due to aforementioned 3D flow patterns encountered inside the cavity. As a result of momentum losses of the fluid front and back cavity walls as well as complex fluid patterns, the temperature field also becomes three-dimensional.

Table 3. Comparisons of the mean Nusselt numbers computed from 2D and 3D models for W/D=0.5 and H/D=1

Re	Ri	Nu_{2D}	Nu_{3D}
10	0.1	1.13	1.15
10	1	1.13	1.15
10	10	1.14	1.17
100	0.1	1.69	1.72
100	1	1.75	1.79
100	10	3.44	2.49
200	0.1	1.99	2.05
200	1	2.41	2.56
200	10	5.83	3.38

(a)

(b)

(c)

(d)
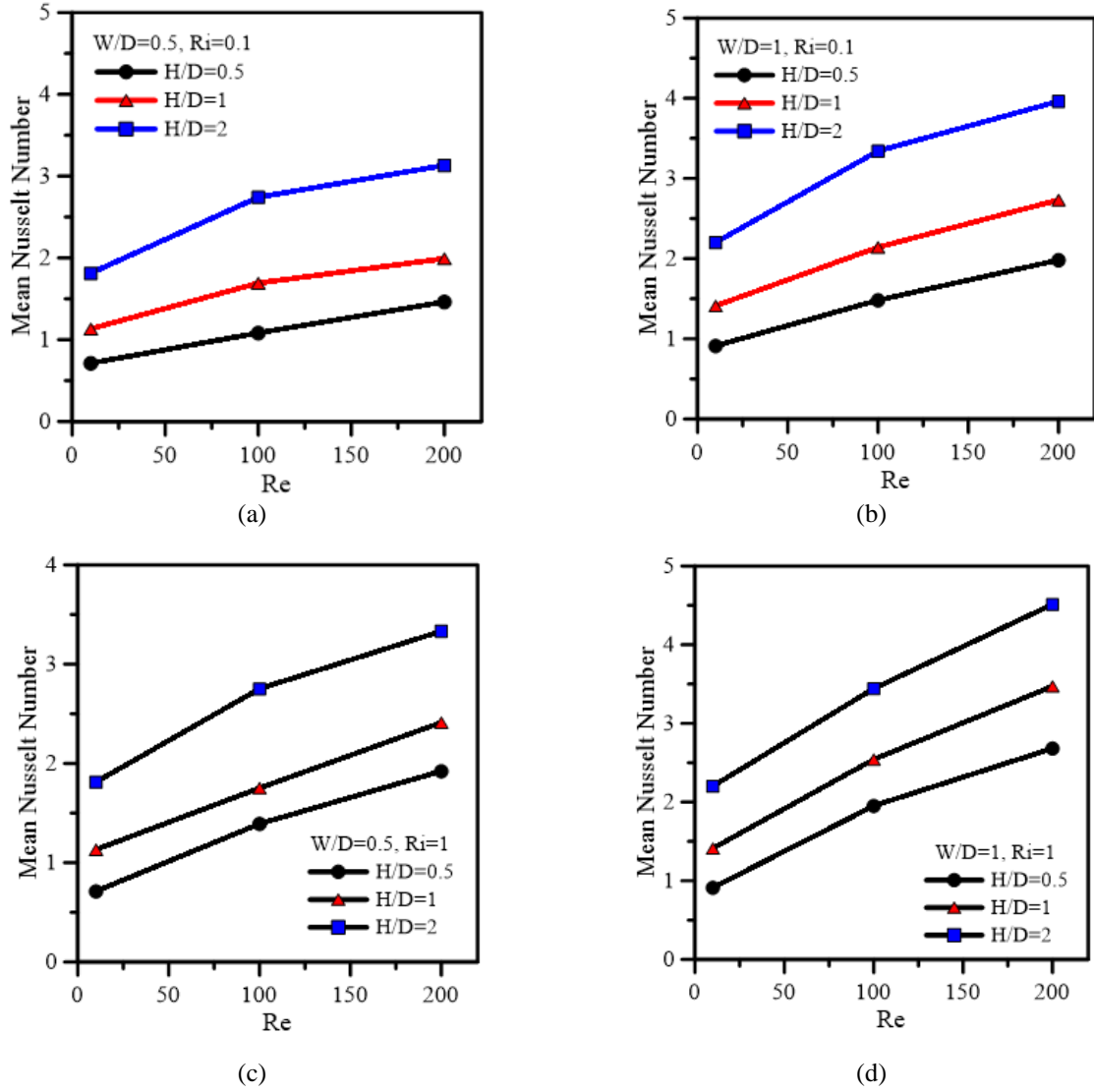
Figure 10. Variation of the computed mean Nusselt number (using 3D models) with the Reynolds number for (a) Ri=0.1, W/D=0.5, (b) Ri=0.1, W/D=1, (c) Ri=1, W/D=0.5, (d) Ri=1, W/D=1.

Heat Transfer Correlations

The mean Nusselt numbers computed from 2D and 3D numerical simulations for all cases and parameters considered in the study were fitted using a regression analysis, and correlations were developed. For 2D simulations, the mean Nusselt number correlation using 144 data sets using four variables led to (Timuralp,2015).

$$\overline{Nu} = 0.674 Re^{0.32} Ri^{0.09} \left(\frac{H}{D}\right)^{0.403} \left(\frac{W}{D}\right)^{0.351}, \quad r^2 = 0.978 \quad (5)$$

for $10 \leq Re \leq 200$, $0.01 \leq Ri \leq 10$, $0.25 \leq \frac{H}{D} \leq 2$, $0.5 \leq \frac{W}{D} \leq 2$

The mean Nusselt number correlation using 54 data sets from three-dimensional numerical simulations using all parameters investigated yields (Timuralp,2015)

$$\overline{Nu} = 0.354 Re^{0.481} Ri^{0.248} \left(\frac{H}{D}\right)^{0.135} \left(\frac{W}{D}\right)^{0.487}, \quad r^2 = 0.949 \quad (6)$$

for $10 \leq Re \leq 200$, $0.1 \leq Ri \leq 10$, $0.5 \leq \frac{H}{D} \leq 2$, $0.5 \leq \frac{W}{D} \leq 1$

CONCLUSIONS

Heat transfer and fluid flow in an open cavity placed below a straight duct are simulated numerically using 2D and 3D models with respect to W/D and H/D, and Richardson and Reynolds numbers. Left surface of the duct is maintained at constant temperature while all other walls, including the duct, are assumed to be adiabatic. The flow through streamlines and/or pathlines and the heat transfer through isotherms and the computed mean Nusselt numbers are studied qualitatively and quantitatively. The study yields the following conclusions:

a) For small W/D cavities, the buoyancy induced circulations are weak, for small Re values, the heat transfer process is dominated by conduction; however, fluid circulations and heat transfer increase with increasing W/D;

b) For large Reynolds numbers and Ri>1, the flow becomes stronger and three-dimensional unstable flow patterns are observed inside the cavity which also

45

effects the mean Nusselt number yielding smaller values than those of computed from 2D models;

c) As the Richardson number is increased, either in 2D or 3D simulations, the mean Nusselt number increases and becomes more pronounced at higher Reynolds number values;

d) For increasing H/D allowing fluid escape from the cavity yields increase in the mean Nusselt number;

e) Two correlations that can be used in practical engineering applications, using 2D and 3D models, were obtained.

REFERENCES

Abdellahoum C., Mataoui A. and Oztop H.F., 2015, Comparison of viscosity variation formulations for turbulent flow of Al2O3-water nanofluid over a heated cavity in a duct, *Advanced Powder Technology*, 26, 1210-1218.

Abdelmassih G., Vernet A. and Pallares J., 2016, Steady and unsteady mixed convection flow in a cubical open cavity with the bottom wall heated, *International Journal of Heat and Mass Transfer*, 101, 682-691.

Aminossadati S.M. and Ghasemi B., 2009, A numerical study of mixed convection in a horizontal channel with a discrete heat source in an open cavity, *European Journal of Mechanics B-Fluid*, 28, 590-598.

Aydin O., Unal A. and Ayhan T., 1999, Natural convection in rectangular enclosures heated from one side and cooled from the ceiling, *International Journal of Heat and Mass Transfer*, 42, 2345-2355.

Basak T., Roy S., Sharma P.K. and Pop I., 2009, Analysis of mixed convection flows within a square cavity with uniform and non-uniform heating of bottom wall, *International Journal of Thermal Sciences*, 48, 891-912.

Brown N.M. and Lai F.C., 2005, Correlations for combined heat and mass transfer from an open cavity in a horizontal channel, *International Communications in Heat and Mass Transfer*, 32, 1000-1008.

Burgos J., Cueta I. and Saluena, C., 2016, Numerical study of laminar mixed convection in a square open cavity, *International Journal of Heat and Mass Transfer*, 99, 599-612.

Calcagni B., Marsili F. and Paroncini M., 2005, Natural convective heat transfer in square enclosures heated from below, *Applied Thermal Engineering*, 25, 2522-2531.

Chang T.S. and Tsay Y.L., 2001, Natural convection heat transfer in an enclosure with a heated backward step, *International Journal of Heat and Mass Transfer*, 44, 3963-3971.

Das S.P., Chakraborty S. and Dutta P., 2002, Natural convection in a two-dimensional enclosure heated symmetrically from both sides, *International Communications in Heat and Mass Transfer*, 29, 345-354.

Erturk E., Corke T.C. and Gokcol C., 2005, Numerical solutions of 2-D steady incompressible driven cavity flow at high Reynolds numbers, *International Journal for Numerical Methods in Fluids*, 48, 747-774.

Fluent, FLUENT 6.3 User's Guide, FLUENT Inc, Lebanon, NH, 2003.

Freitas C.J. and Street R.L., 1988, Non-Linear Transient Phenomena in a Complex Recirculating Flow - a Numerical Investigation, *International Journal for Numerical Methods in Fluids*, 8, 769-802.

Ishihara I., Fukui T. and Matsumoto R., 2002, Natural convection in a vertical rectangular enclosure with symmetrically localized heating and cooling zones, *International Journal of Heat Fluid Flow*, 23, 366-372.

Iwatsu R. and Hyun J.M., 1995, Three-dimensional Driven-Cavity Flows with a Vertical Temperature-Gradient, *International Journal of Heat and Mass Transfer*, 38, 3319-3328.

Khanafer K.M. and Chamkha A.J., 1999, Mixed convection flow in a lid-driven enclosure filled with a fluid-saturated porous medium, *International Journal of Heat and Mass Transfer*, 42, 2465-2481.

Leong J.C., Brown N.M. and Lai F.C., 2005, Mixed convection from an open cavity in a horizontal channel, *International Communications in Heat and Mass Transfer*, 32, 583-592.

Manca O., Nardini S., Khanafer K. and Vafai K., 2003, Effect of heated wall position on mixed convection in a channel with an open cavity, *Numerical Heat Transfer Part a-Applications*, 43, 259-282.

Manca O., Nardini S. and Vafai K., 2006, Experimental investigation of mixed convection in a channel with an open cavity, *Experimental Heat Transfer*, 19, 53-68.

Manca O., Nardini S. and Vafai K., 2008, Experimental investigation of opposing mixed convection in a channel with an open cavity below, *Experimental Heat Transfer*, 21, 99-114.

Mehrez Z., Bouterra M., El Cafsi A. and Belghith A., 2013, Heat transfer and entropy generation analysis of nanofluids flow in an open cavity, *Computers & Fluids*, 88, 363-373.

Mehrez Z., El Cafsi A., Belghith A. and Le Quéré P., 2015,The entropy generation analysis in the mixed convective assisting flow of Cu–water nanofluid in an

inclined open cavity, *Advanced Powder Technology*, 25, 1442-1451.

Moallemi M.K. and Jang K.S., 1992, Prandtl Number Effects on Laminar Mixed Convection Heat-Transfer in a Lid-Driven Cavity, *International Journal of Heat and Mass Transfer*, 35, 1881-1892.

Mohamad A.A. and Viskanta R., 1991, Transient Low Prandtl Number Fluid Convection in a Lid-Driven Cavity, *Numerical Heat Transfer Part A-Applications*, 19, 187-205.

Mohamad A.A. and Viskanta R., 1995, Flow and Heat-Transfer in a Lid-Driven Cavity Filled with a Stably Stratified Fluid, *Applied Mathematical Modelling*, 19, 465-472.

Muftuoglu A. and Bilgen E., 2008, Natural convection in an open square cavity with discrete heaters at their optimized positions, *International Journal of Thermal Sciences*, 47, 369-377.

Pallares J., Cuesta I., Grau F.X. and Giralt F., 1996, Natural convection in a cubical cavity heated from below at low Rayleigh numbers, *International Journal of Heat and Mass Transfer*, 39, 3233-3247.

Prasad A.K. and Koseff J.R., 1996, Combined forced and natural convection heat transfer in a deep lid driven cavity flow, *International Journal of Heat and Fluid Flow*, 17, 460-467.

Rahman M.M., Oztop H.F., Rahim N.A., Saidur R., Al-Salem K., Amin N., Mamun M.A.H. and Ahsan A., 2012, Computational analysis of mixed convection in a channel with a cavity heated from different sides, *International Communications in Heat and Mass Transfer*, 39, 78-84.

Selimefendigil F. and Yurddas A., 2012, Numerical Analysis of Mixed Convection Heat Transfer in Pulsating Flow for a Horizontal Channel with a Cavity Heated from Vertical Side and Below, *Heat Transfer Research*, 43, 509-525.

Sharif M.A.R., 2007, Laminar mixed convection in shallow inclined driven cavities with hot moving lid on top and cooled from bottom, *Applied Thermal Engineering*, 27, 1036-1042.

Sidik N.A.C., Jahanshaloo L. and Safdari A., 2014, The effect of mixed convection on particle laden flow analysis in a cavity using a Lattice Boltzmann method, *Computers & Mathematics with Applications*, 67, 52-61.

Stiriba Y., 2008, Analysis of the flow and heat transfer characteristics for assisting incompressible laminar flow past an open cavity, *International Communications in Heat and Mass Transfer*, 35, 901-907.

Stiriba Y., Ferre J.A. and Grau F.X., 2013, Heat transfer and fluid flow characteristics of laminar flow past an open cavity with heating from below, *International Communications in Heat and Mass Transfer*, 43, 8-15.

Stiriba Y., Grau F.X., Ferre J.A. and Vernet A., 2010, A numerical study of three-dimensional laminar mixed convection past an open cavity, *International Journal of Heat and Mass Transfer*, 53, 4797-4808.

Timuralp C., 2015, Investigation of the two and three dimensional heat transfer and fluid flow in a channel with an open cavity, Ph. D Thesis, Eskisehir Osmangazi University, Eskisehir, Turkey.